PHYSICAL REVIEW C VOLUME 24, NUMBER 4 OCTOBER 1981

Interacting boson approximation description of the collective states of ^{168}Er and a comparison with geometrical models

D. D. Warner and R. F. Casten
Brookhaven National Laboratory, Upton, New York 11973

W. F. Davidson
National Research Council of Canada, Ottawa, Ontario K1A OR6, Canada

(Received 8 April 1981)

The interacting boson approximation has been used to calculate the positive parity states of ^{168}Er below 2 MeV. A simple parametrization has been used which corresponds to a description close to the SU(3) limit of the model. The predictions have been compared with new results available from a recent experimental study. Particular attention has been paid to the absolute magnitude of predicted $B(E2)$ values in assessing the significance of discrepancies between theory and experiment. Estimates of absolute strengths have also been obtained for $M1$ transitions in the scheme. The calculations correctly reproduce the complete sequence of $K^\pi = 0^+$ and 2^+ bands below the pairing gap and provide an excellent overall description of their decay properties. Most importantly, the predicted dominance of the decay from the β to the γ band, over that to the ground state band, which represents a fundamental characteristic of the model in this region, is reflected by the experimental data. The reproduction of this feature from a band mixing approach in the framework of the geometrical description is also discussed, and the connection between the two descriptions is explored.

[NUCLEAR STRUCTURE Interacting boson approximation applied to ^{168}Er. Calculated levels, $B(E2)$, branching ratios. Single particle estimates of $B(M1)$, $B(E2)$. Comparison with experimental and band-mixing formalism in rotational model.]

I. INTRODUCTION

In the past few years, considerable effort has been applied to test the predictions of the interacting boson approximation (IBA)[1] over a wide range of nuclei, and the results have shown[2] that the model represents a very significant step forward in the description of collective nuclear excitations. The underlying SU(6) group structure of the model basis leads to a simple Hamiltonian which is capable of describing both the three specific types of collective structure with classical geometrical analogs (vibrational, rotational, and γ unstable) and the transitional nuclei whose structures are intermediate. In addition, the three geometrical descriptions emerge naturally as subgroups of SU(6) with specific symmetries, such that vibrational, rotational, and γ-unstable nuclei correspond to the SU(5), SU(3), and O(6) limits of the IBA Hamiltonian.

Probably the most familiar and well understood of the geometrical descriptions is that of the symmetric rotor,[3] corresponding to the SU(3) limit in the IBA, and thus, a detailed study of the model in a situation close to this limit should facilitate an overall understanding of the correspondences and differences between the two descriptions, which will then be applicable to a broad class of nuclei. In this respect, it should be noted that while for any particular limiting symmetry of the IBA, the predicted structure is very similar to that of the corresponding geometrical limit, there are specific differences which result from the symmetry of the IBA Hamiltonian, from the explicit inclusion of

the finite number of valence particles, and from the adoption of a basis incorporating only pairs of valence particles coupled to $L = 0$ and 2. Indeed, questions raised concerning the validity of this latter assumption in the presence of a deformed field[4] have recently led to considerable controversy, and thus the region of deformed nuclei represents a particularly crucial testing ground for the IBA at this time.

The extent to which any model can be tested depends on the amount of experimental information available and, in particular, on the degree of completeness of that information. Level schemes established from reactions which populate states with a specific type of structure leave open the possibility that some states have not been identified, and hence, the correspondence between theory and experiment may not be unambiguous. The (n,γ) reaction to a large extent overcomes these problems, since its nonspecific nature ensures the population of broad classes of states, irrespective of their structure. In particular, the recent combination of the techniques of curved crystal spectrometry and average resonance capture (ARC) in such (n,γ) studies has led to the establishment of level schemes with certain unique attributes.[5] The high resolution and sensitivity of the curved crystal spectrometer data provide a great wealth of information on the decay of the levels and, most importantly, permit the identification of weak, low energy transitions which deexcite levels at high excitation energy and which, therefore, frequently represent the dominant collective decay modes of such levels. The use of the ARC technique can provide a unique *guarantee* that *all* levels within a given spin and excitation range have been identified.

The results of such studies have already led to perhaps the most thorough test of the predictions of the IBA to date, namely that for the Pt-Os nuclei[6] which represent the transition from the O(6) limit evidenced in ^{196}Pt, towards the SU(3) limit expected in midshell. A more recent investigation of the ^{167}Er$(n,\gamma)^{168}$Er reaction[7] with the same techniques has led to the establishment of a level scheme for ^{168}Er, shown in Fig. 1, which is undoubtedly the most detailed and complete level scheme currently available for an even mass deformed nucleus. This detail is exemplified in Fig. 2, where the decay of the ground, γ, and first two excited 0^+ bands are shown. It can be remarked that, in the case of the γ band, 28 out of the 29 deexciting transitions which are possible, simply

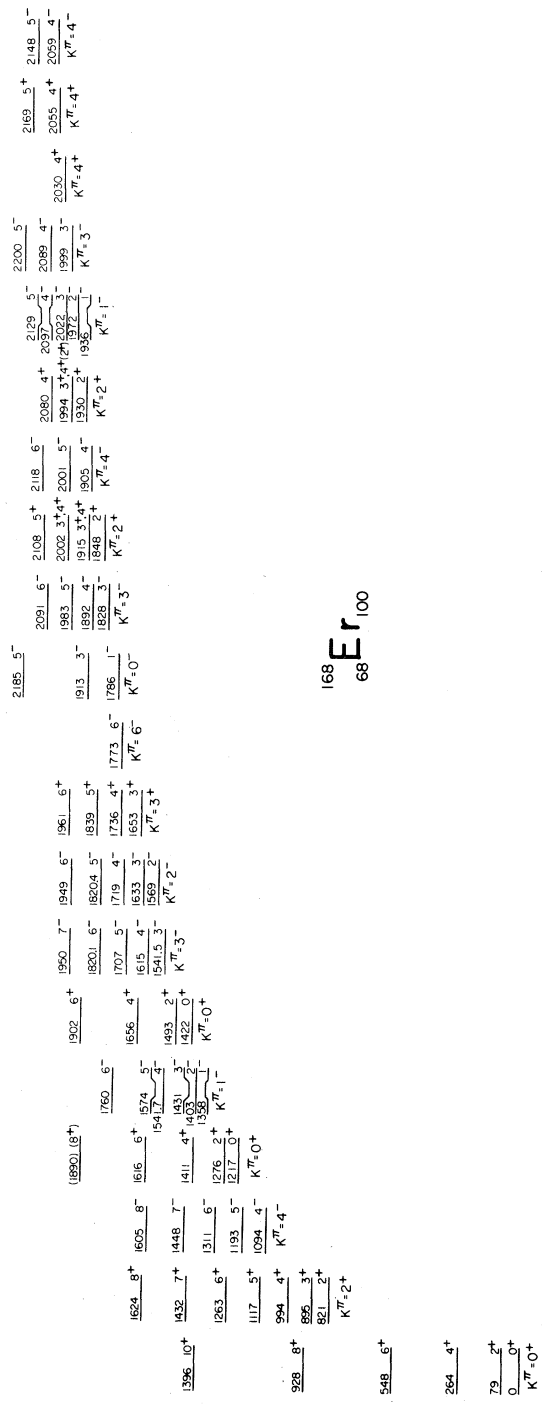

FIG. 1. The complete set of levels identified in ^{168}Er in the study of Ref. 7.

from spin considerations, have been identified. In addition, the overall level scheme is *known to be complete* for all levels with $J < 6$ and $E_x < 2$ MeV. These data thus offer a unique opportunity to in-

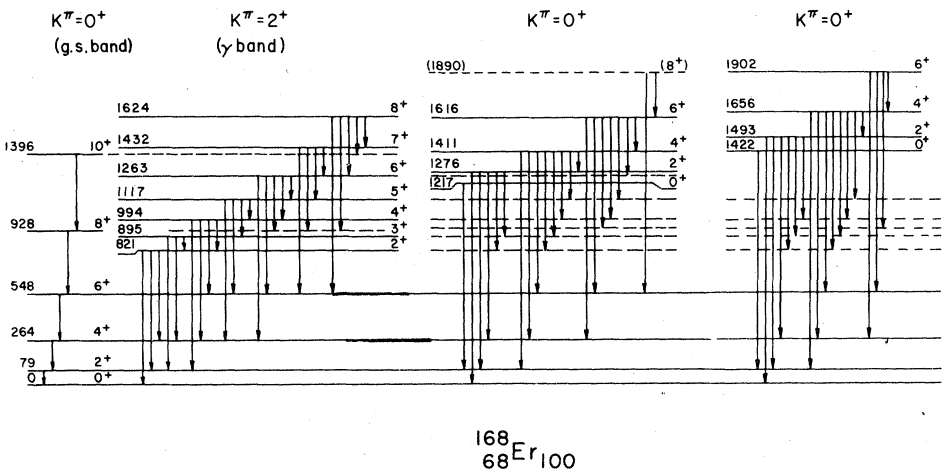

FIG. 2. A portion of the experimental level scheme of ^{168}Er based upon the results of Ref. 7. The deexcitation modes of the ground state band, gamma band, and the two 0^+ bands are shown.

vestigate the applicability of the IBA model to a well deformed nucleus, and hence, to study the specific characteristics of the SU(3) limit of the model. Some of the principal results have already been briefly reported elsewhere.[8] The current study is also aimed at exploring the relationship of such an IBA description to the parallel one which could be obtained in a geometrical framework,[3] and at quantifying, to some extent, the departures from pure collectivity evidenced by the data.

In order to highlight the effects of the SU(3) symmetry, and to clarify the connection of the IBA in this limit with the familiar concepts of the symmetric rotor, the perturbation to the rigorous limit has been kept as simple as possible. The resulting comparison between the two descriptions is discussed in Sec. V.

II. IBA CALCULATIONS

A. Energies

The calculations have been performed with the code PHINT (IBA-1)[9] and hence, no distinction has been made between neutron and proton bosons. The number of bosons implied by the number of valence neutrons and protons in ^{168}Er is 16 and the resulting number of basis states involved is thus large. The inclusion of an f boson, to generate negative parity states, then produces a severe computational problem in terms of the dimensions of the matrices which must be diagonalized. In addition, given the transfer reaction data available for this nucleus, the identification of a set of purely collective octupole vibrational bands is difficult, and it seems likely that the candidates for such excitations may be significantly perturbed by interactions with known two quasiparticle configurations. Such perturbations lie outside the basis of the IBA, and hence, for these reasons, the calculations have been limited to the positive parity bands below the pairing gap, estimated as 2 MeV. Note that in the discussion which follows, the familiar terminology of "β" and "γ" bands is used to describe the lowest excited $K^\pi = 0^+$ and 2^+ bands predicted by the model, although, as will be seen later, such a description is not precise.

In keeping with the simple approach mentioned previously, a truncated multipole expansion of the IBA Hamilton was used in the calculations, namely

$$H = -\kappa Q\cdot Q - \kappa' L\cdot L + \kappa'' P\cdot P \ . \tag{1}$$

The obvious starting point in an IBA description of a well deformed nucleus is the SU(3) limit, which describes a symmetric rotor with degenerate β and γ bands. This limit arises naturally from the Hamiltonian of Eq. (1) when the last term is zero. In such a case, the energies of states can be described by the expression

$$E = (0.75\kappa - \kappa')J(J+1) - \kappa C(\lambda,\mu) \ , \tag{2}$$

where $C(\lambda,\mu)$ is the eigenvalue of the Casimir

operator.[1] The first term of Eq. (2) describes the spacings within rotational bands, while the second, dependent only on the $Q\cdot Q$ interaction, determines the intrinsic energies of the collective bands. Thus the parameters κ and κ' in the SU(3) limit can be extracted from the energy of the first 2^+ state, which depends only on the first term of Eq. (2), and from the energy difference of the second and first 2^+ states, which depends only on the second term. The eigenvalue of the Casimir operator is given by

$$C(\lambda,\mu) = \lambda^2 + \mu^2 + \lambda\mu + 3(\lambda + \mu) . \tag{3}$$

The ground band representation is denoted by (λ,μ) while the next representation, $(\lambda - 4,2)$, includes the β and γ bands of the geometrical description. Then, Eqs. (2) and (3) lead to

$$\kappa = [E(2_2^+) - E(2_1^+)]/6(\lambda - 1) ,$$
$$\kappa' = 0.75\kappa - E(2_1^+)/6 , \tag{4}$$

where λ is the number of valence *particles* in the nucleus.

In the case of ^{168}Er, any perturbation to the rigorous SU(3) limit described above can be expected to lie in the direction of the O(6) limit, which occurs towards the end of the shell. The following procedure was therefore adopted in the current calculations. The parameters κ and κ' were calculated from the energies of the 2_1^+ and 2_2^+ states, as described in Eq. (4). This results in a level scheme in which the ground and γ bands are well reproduced, but in which the β band is degenerate with the γ band, and in which the higher lying bands lie in degenerate groups also, corresponding to the multiphonon excitations $\beta\gamma$, $\gamma\gamma$, etc.) of the geometrical model. Clearly, from Figs. 1 and 2, this does not correspond to the situation in ^{168}Er. The pairing term of Eq. (1), which is important in the O(6) limit, was then introduced, and the parameter κ'' varied to obtain the final calculated sequence of levels. It should be emphasized, therefore, that the complete sequence of predicted bands results effectively from the variation of *a single parameter* given that κ and κ' were fixed from two experimental energies. *No further attempt to improve the agreement between theory and experiment was made* since the philosophy of this calculation was to investigate the validity of the IBA in a situation as close as possible to the SU(3) limit.

B. $B(E2)$ values

The $E2$ operator in the IBA is given by

$$T(E2) = \alpha(d^\dagger s + s^\dagger \tilde{d})^{(2)} + \frac{\beta}{\sqrt{5}}(d^\dagger \tilde{d})^{(2)} . \tag{5}$$

Relative $B(E2)$ values thus depend on one parameter, the ratio of β/α, while absolute $B(E2)$ values depend on the absolute magnitude of α. In the SU(3) limit, the ratio is -2.958, and in this limit, the operator of Eq. (5) cannot connect states belonging to different representations (λ,μ). In the O(6) limit, the ratio of β/α is zero, and hence, for ^{168}Er it can be expected to lie between the two limiting values. In the present calculation, no attempt was made to optimize this ratio. Instead, the measured values[10] of $B(E2;0_1^+ \rightarrow 2_1^+)$ and $B(E2;0_1^+ \rightarrow 2_2^+)$ were used to calculate absolute and unique values of β and α. This procedure yielded a ratio of -0.68, and allowed absolute $B(E2)$ values to be calculated for all transitions. Thus it should be emphasized that there were *no free parameters* associated with the calculation of any other $B(E2)$ values in this study.

While the experimental information available from the (n,γ) study involves, of course, branching ratios and thus relative $B(E2)$ values, the extraction of absolute $B(E2)$ values in the IBA calculation by the procedure mentioned above enabled the predicted single particle strength of the collective $E2$ transitions to be estimated. The Weisskopf estimate[11] for the matrix element of a single proton transition was used, namely

$$\langle f \,|\, T(E2) \,|\, i \rangle^2 \approx \frac{9e^2}{100\pi} R^4 , \tag{6}$$

where R, the nuclear radius, was taken as $1.2A^{1/3}$ fm. This gives a value of 0.0269 e^2b^2 for the $B(E2;0^+ \rightarrow 2^+)$ single particle unit (s.p.u.) in ^{168}Er. In addition, to facilitate comparison of the strengths of branches to different bands, the square of the appropriate Clebsch-Gordan coefficient has been divided out to yield, for each transition, a value for the square of the effective intrinsic matrix element, i.e.,

$$\langle K_f \,|\, M'(E2) \,|\, K_i \rangle^2 = B(E2;\, I_iK_i \rightarrow I_fK_f)/\langle I_i 2K_iK_f - K_i \,|\, I_fK_f \rangle^2 \times \begin{cases} 2 \text{ if } |K_i - K_f| = 2 \\ 1 \text{ if } |K_i - K_f| = 0 . \end{cases} \tag{7}$$

Note that the last factor in the denominator of the right hand side of Eq. (7) takes account of the cross terms involved in transitions between $K = 0$ and 2 bands.

III. RESULTS

A. Energies

The calculated level structure of ^{168}Er is compared with experiment in Fig. 3, and it can be seen that the entire experimental sequence of states below the pairing gap (2 MeV) has been well reproduced. Note that although, for convenience, the bands have been labeled by K quantum numbers, there is no assumption of K quantum number inherent in the IBA basis. Nevertheless, level sequences corresponding to ground, β, and γ bands appear, as well as sequences which, in a geometrical description, would be labeled as multiphonon excitations. The IBA wave functions can, of course, be expressed in terms of a basis involving a K quantum number but it is interesting to note that such a transformation results in finite admixtures between different (pure K) bands, even in the rigorous SU(3) limit.[1] These and other aspects of the correspondence between the IBA and geometrical descriptions will be discussed in more detail in Sec. V.

Thus, given the *known completeness* of the experimental level scheme mentioned earlier, it can be stated that all empirical bands below the pairing gap are predicted. The one exception to this is a $K^\pi = 3^+$ band at 1653 keV which, by definition, lies outside the basis of a description incorporating only $L = 0$ and 2 bosons. The origin of such a band could be from quasiparticle excitations, or alternately, could be described by the introduction of a g boson ($L = 4$) into the IBA basis. It is, therefore, outside the scope of the present investigation although the consequences of its introduction and in particular the interaction of levels originating from the g boson with those of the s-d boson basis is an important question.[12]

Despite the excellent overall agreement between theory and experiment, certain discrepancies emerge near the pairing gap. In particular, the highest lying $K^\pi = 2^+$ band is predicted at too high an energy, while the calculation also predicts a

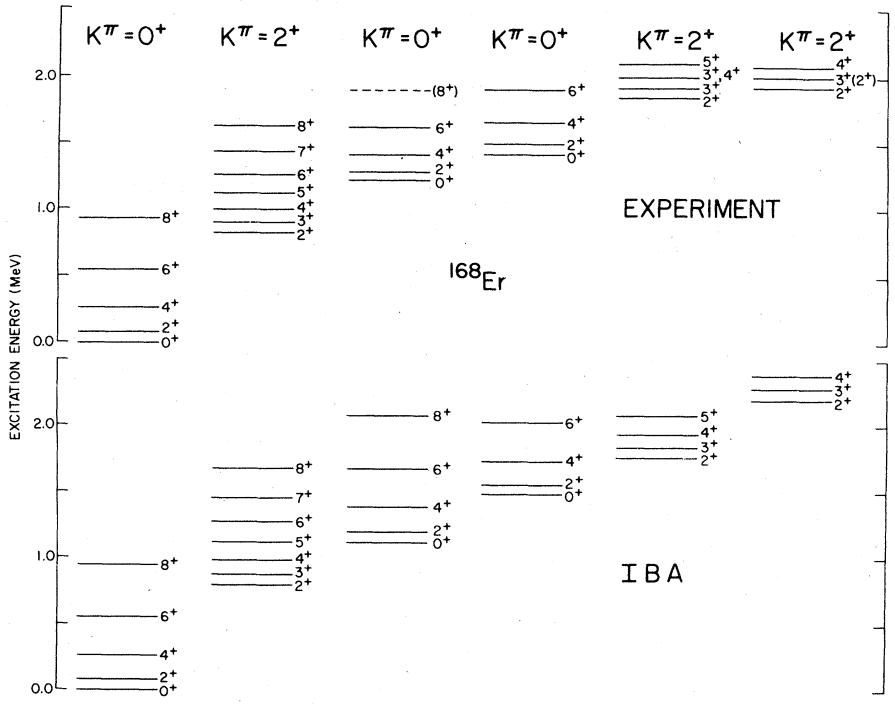

FIG. 3. Levels in ^{168}Er compared with the results of the IBA calculation. All $K^\pi = 0^+$ and 2^+ bands with experimental bandheads below the pairing gap (2 MeV) have been shown. The constants κ and κ' of Eq. (1) were fixed according to the prescription of Eq. (4), and the resulting values are 0.004 and -0.0105 MeV, respectively. The parameter κ'' was the only one varied to optimize the fit to experimental energies, and the adopted value is 0.015 MeV. The $K^\pi = 3^+$ and 4^+ bands are not shown (see text).

$K^\pi = 4^+$ band at 1619 keV, whereas the lowest lying 4^+ band found experimentally is at 2030 keV. The appearance of these discrepancies is probably not surprising since, at excitation energies near the pairing gap, interactions with two quasiparticle degrees of freedom are likely to perturb the purely collective description offered by the IBA. In addition, and as mentioned earlier, the restriction of the IBA basis to only $L = 0$ and 2 bosons may eventually become inadequate at higher excitation energies. In particular, the incorporation of a g boson in the scheme, necessary to generate the $K^\pi = 3^+$ band at 1653 keV, might also account for the discrepancy in the $K^\pi = 4^+$ band energy, since the g boson is predicted to interact strongly with this band. The (d,d') data of Ref. 13 shows that the 4^+ member of the $K^\pi = 3^+$ band is indeed populated with significant strength, while the (d,p) data of Ref. 14 shows no significant population of this band. Both sets of data thus support a collective interpretation.

There is one other general discrepancy which should be mentioned, namely the failure of the calculation to reproduce the changes in the moment of inertia between different bands. This feature is, in fact, inherent in the decision to employ the simple truncated Hamiltonian of Eq. (1), since such a formalism results in almost constant rotational spacing for each band. Thus the reproduction of, for instance, the 25% increase in the moment of inertia of the β band is outside the scope of the treatment presented here. However, it should be noted that the production of bands with differing moments of inertia is not outside the scope of the IBA model in general. Such effects might be produced by adding other perturbations to the Hamiltonian or by introducing higher order terms.

B. $B(E2)$ values

Inspection of Table I shows that the agreement between theory and experiment for transitions originating within the γ band is excellent. Not surprisingly, the calculated relative $B(E2)$ values between intraband transitions or between interband transitions alone follow closely the predictions of the Alaga rules.[16] Thus, although the rigorous SU(3) symmetry has been broken by the introduction of the $P\cdot P$ term into the Hamiltonian, so that, for example, the β and γ bands are no longer degenerate, the wave functions are still not greatly different from those of the SU(3) limit, and hence, in a geometrical description, the bands can still be thought of as having good K quantum numbers. The important additional achievement of the IBA calculation is the correct reproduction of the ratio of *intraband to interband* strengths, which depend on the relative *intrinsic* matrix elements between the bands. This feature depends mostly on the relative sizes of the two terms in the $E2$ operator of Eq. (5), rather than on the perturbation applied to the SU(3) Hamiltonian. The only significant discrepancy is that for the $8^+_\gamma \rightarrow 7^+_\gamma$ intraband transition which has a much greater measured intensity than predicted. However, this transition is very weak experimentally, with an intensity error of 50%. Also, no multipolarity determination could be made, and hence, the $M1$ component is unknown.

The results of the $B(E2)$ calculations for transitions from the β band are given in Table II. It can be seen that the overall agreement is again good, although not as prescise as for the γ band. In particular, the predicted intensities of the transitions from the 4^+ state to the 4^+_γ and 5^+_γ states are severely overestimated. However, the most impressive success of the calculation is again the reproduction of the overall observed branches between bands, which span three orders of magnitude. One crucial feature is evident, namely that the branch to the γ band is larger than that to the ground band, in both theory and experiment. This dominance is particularly significant, since it arises naturally in the IBA calculation as a result of the fact that in the SU(3) limit the β and γ bands both belong to the same SU(3) representation, and this representation is different from that of the ground band; hence, transitions between the β and ground bands are forbidden. Thus, while the small perturbation applied in the present calculations breaks this symmetry to allow transitions to the ground band, the dominance of the branch to the γ band still remains. The *degree* of this dominance, however, as mentioned earlier, depends strongly on the ratio of the two coefficients of the $E2$ operator. The closer this ratio is to the SU(3) value of -2.958, the greater the predicted dominance of intra-representation over inter-representation transitions. Conversely, in the pure geometrical description, the intrinsic $E2$ matrix element between β and γ bands must be zero, since the transition would require the destruction of one type of vibration and the creation of a different type. However, as pointed out earlier, the IBA description, even in the SU(3) limit, is related to a geometrical descrip-

TABLE I. Comparison of experimental and theoretical $B(E2)$ branching ratios from states of the gamma band in ^{168}Er.

Transition[a]		Calculated absolute	Calculated	Relative $B(E2; I_i \rightarrow I_f)$	
I_i^π	I_f^π, K	$B(E2; I_i \rightarrow I_f)$ (s.p.u.)	$\langle K_f \mid M'(E2) \mid K_i \rangle^{2}$[b] (s.p.u.)	IBA	Exp.[c]
2^+	$0^+,0$	1.02	2.05	66.0	54.0
	$2^+,0$	1.55	2.71	100.0	100.0
	$4^+,0$	0.09	3.10	6.0	6.8
3^+	$2^+,0$	1.80	2.52	2.7	2.6
	$4^+,0$	0.85	2.97	1.3	1.7
	$2^+,2$	66.23	185.0	100.0	100.0
4^+	$2^+,0$	0.55	2.29	2.5	1.6
	$4^+,0$	1.85	2.63	8.3	8.1
	$6^+,0$	0.22	3.54	1.0	1.1
	$2^+,2$	22.08	184.0	100.0	100.0
5^+	$4^+,0$	1.49	2.34	4.3	2.9
	$6^+,0$	1.10	3.03	3.1	3.6
	$3^+,2$	35.04	183.0	100.0	100.0
	$4^+,2$	34.51	181.0	98.5	122.0
6^+	$4^+,0$	0.41	2.11	0.97	0.44
	$6^+,0$	1.83	2.52	4.3	3.8
	$8^+,0$	0.31	4.01	0.73	1.4
	$4^+,2$	42.75	182.0	100.0	100.0
	$5^+,2$	25.17	179.0	59.0	69.0
7^+	$6^+,0$	1.29	2.15	2.7	0.74
	$5^+,2$	47.19	179.0	100.0	100.0
	$6^+,2$	18.58	172.0	39.0	59.0
8^+	$6^+,0$	0.33	1.88	0.67	1.8
	$8^+,0$	1.74	2.36	3.5	5.1
	$6^+,2$	50.14	177.0	100.0	100.0
	$7^+,2$	14.49	170.0	29.0	135.0

[a] The $4_\gamma^+ \rightarrow 3_\gamma^+$ transition was not observed in the measurement and no meaningful limit on its intensity could be extracted, since it was obscured by a strong line of similar energy. The $7_\gamma^+ \rightarrow 8_g^+$ transition was measured to be of pure $M1$ multipolarity. Thus both these transitions have been excluded from this comparison.

[b] This column lists the squares of the intrinsic matrix elements in s.p.u. extracted from the IBA calculations according to Eq. (7).

[c] For all $\Delta I = 0$ or 1 transitions, up to and including the $7_\gamma^+ \rightarrow 6_g^+$, multipolarities have been determined and measured $M1$ components subtracted (Refs. 7 and 15). All other transitions have been assumed to be pure $E2$.

tion incorporating finite admixtures between bands. It is thus of considerable interest to investigate whether, and how, a calculation involving band-mixing in the geometrical formalism can reproduce this feature; this point will be dealt with in detail in Sec. V.

The experimental information concerning decays from the 0_3^+ band is not as complete as for the lower band, and hence, the comparison between theory and experiment, given in Table III, includes a large number of upper limits on intensities which have been extracted from the experimental data of Ref. 7. While the overall agreement seems to be fair, one notable discrepancy seems to be that the experimental branches to the ground band are significantly stronger than predicted. However, in

TABLE II. Comparison of experimental and theoretical $B(E2)$ branching ratios from states of the 0_2^+ band in ^{168}Er.

Transition[a]		Calculated absolute	Calculated	Relative $B(E2;I_i \rightarrow I_f)$	
I_i^π	I_f^π, K	$B(E2;I_i \rightarrow I_f)$ (s.p.u.)	$\langle K_f \mid M'(E2) \mid M_i \rangle^2$[b] (s.p.u.)	IBA	Exp.[c]
0^+	$2^+,0$	0.19	0.19	5.5	5.5
	$2^+,2$	3.36	1.68	100.0	<28.0
2^+	$0^+,0$	0.03	0.17	0.10	0.23
	$4^+,0$	0.11	0.21	0.32	1.4
	$2^+,2$	0.87	1.53	2.6	4.0
	$3^+,2$	1.66	1.66	4.9	$\equiv 4.9$
	$0^+,0'$	33.75	169.0	100.0	
4^+	$2^+,0$	0.04	0.14	0.09	0.02
	$6^+,0$	0.11	0.24	0.23	0.11
	$2^+,2$	0.02	1.16	0.04	0.03
	$3^+,2$	0.30	1.33	0.63	0.35
	$4^+,2$	1.04	1.48	2.2	0.52
	$5^+,2$	1.32	1.70	2.8	0.19
	$2^+,0'$	47.47	166.0	100.0	100.0
6^+	$4^+,0$	0.04	0.12	0.07	0.02
	$8^+,0$	0.11	0.25	0.21	0.07
	$4^+,2$	0.05	1.06	0.09	0.11
	$5^+,2$	0.38	1.22	0.73	0.32
	$6^+,2$	1.02	1.41	2.0	0.93
	$4^+,0'$	51.35	163.0	100.0	100.0

[a] The $I \rightarrow I$ transitions to the ground band were all measured to be of pure $M1$ multipolarity, and these transitions have, therefore, been excluded from this comparison. The notation $0'$ refers to the 0_2^+ band.

[b] This column lists the squares of the intrinsic matrix elements in s.p.u. extracted from the IBA calculations according to Eq. (7).

[c] No multipolarity determinations could be made for the $2^+ \rightarrow 2_\gamma^+$ and $2^+ \rightarrow 3_\gamma^+$ transitions, which have, therefore, been assumed to be pure $E2$ in this comparison. No meaningful limit could be obtained for the $2^+ \rightarrow 0^+$ intraband transition, and hence, the $2^+ \rightarrow 3_\gamma^+$ has been used for normalization in this case.

judging the implications of this discrepancy, the predicted absolute $E2$ strengths should be considered. It can be seen from Table III that the ground state transitions are calculated to have strengths of $\sim 10^{-3}$ to 10^{-2} s.p.u. Thus , the IBA predicts that, in the purely collective basis, these transitions are strongly hindered, and hence, relatively minor perturbations to this pure collective description may well be sufficient to account for the observed discrepancies. This conclusion is, to a certain extent, supported by consideration of the $I \rightarrow I$ transitions between both 0^+ bands and the ground band, where multipolarities have been determined to be essentially pure $M1$ from the experimental data. A first impression might be that such $M1$ transitions represent significant discrepancies between theory and experiment and actually throw some doubt on the overall validity of a collective interpretation for these bands. However, in the next section, it will be shown that these transitions correspond to $M1$ strengths of $\sim 10^{-4}$ s.p.u., and thus, that they do not indicate any significant departure from collectivity, but rather arise because of the weakness of the competing $E2$ modes.

In order to facilitate the overall comparison between theory and experiment for $B(E2)$ branching ratios, and to illuminate the *essential* feature, namely, the prediction of *relative branches to different bands,* it is useful to consider the summed $B(E2)$ strength from a given initial state to all states in a particular final band. These sums are plotted for the γ band in Fig. 4, and for the two 0^+ bands in Fig. 5. In the case of the γ band, it can be seen that the overall intraband to interband branching is excellently reproduced in all cases.

TABLE III. Comparison of experimental and theoretical $B(E2)$ branching ratios from states of the 0_3^+ band in ^{168}Er.

Transition[a]		Calculated absolute	Calculated	Relative $B(E2;I_i \rightarrow I_f)$	
I_i^π	I_f^π,K	$B(E2;I_i \rightarrow I_f)$ (s.p.u.)	$\langle K_f \mid M'(E2) \mid K_i \rangle^{2}$[b] (s.p.u.)	IBA	Exp.[c]
0^+	$2^+,0$	0.01	0.01	0.43	$\equiv 0.43$
	$2^+,2$	2.79	1.40	100.0	< 0.8
	$2^+,0'$	0.01	0.01	0.46	< 59.0
2^+	$0^+,0$	0.002	0.01	0.006	0.09
	$4^+,0$	0.007	0.01	0.02	1.0
	$2^+,2$	0.74	1.30	2.3	1.4
	$3^+,2$	1.38	1.38	4.3	2.0
	$4^+,2$	0.66	1.52	2.0	$\equiv 2.0$
	$0^+,0'$	0.001	0.007	0.004	< 7.0
	$2^+,0'$	0.004	0.01	0.01	< 7.0
	$4^+,0'$	0.009	0.02	0.03	< 3000.0
	$0^+,0''$	32.24	161.0	100.0	< 4000.0
4^+	$2^+,0$	0.002	0.008	0.005	0.01
	$6^+,0$	0.007	0.015	0.01	0.34
	$2^+,2$	0.02	1.15	0.04	0.08
	$3^+,2$	0.26	1.17	0.58	0.08
	$5^+,2$	1.08	1.40	2.4	0.48
	$6^+,2$	0.48	1.69	1.1	< 0.4
	$2^+,0'$	0.001	0.004	0.002	< 4.0
	$4^+,0'$	0.007	0.025	0.01	< 3.0
	$2^+,0''$	45.47	159.0	100.0	100.0
6^+	$4^+,0$	0.002	0.007	0.004	0.05
	$6^+,0$	0.003	0.01	0.006	0.48
	$8^+,0$	0.007	0.02	0.01	0.32
	$5^+,2$	0.34	1.10	0.69	< 0.3
	$6^+,2$	0.86	1.18	1.7	< 40.0
	$7^+,2$	0.97	1.40	2.0	< 0.6
	$8^+,2$	0.44	1.89	0.90	< 6.0
	$4^+,0'$	0.0005	0.002	0.001	< 0.6
	$6^+,0'$	0.01	0.05	0.03	< 6.0
	$4^+,0''$	48.96	155.0	100.0	100.0

[a] The $2^+ \rightarrow 2_g^+$, $4^+ \rightarrow 4_\gamma^+$ transitions have been omitted since their multipolarities were determined to be pure $M1$. In addition, no meaningful limits for the $4^+ \rightarrow 6_3^+$ and $6^+ \rightarrow 4_\gamma^+$ transitons could be extracted from the data and, hence, these have also been excluded. The notation $0',0''$ refers to the 0_2^+ and 0_3^+ bands, respectively.

[b] This column lists the squares of the intrinsic matrix elements in s.p.u. extracted from the IBA calculations according to Eq. (7).

[c] $M1$ components in the $4^+ \rightarrow 5_\gamma^+$ and $6^+ \rightarrow 6_g^+$ transitions have been determined and allowed for. No multipolarity determinations could be made for the $2^+ \rightarrow 2_\gamma^+$ and $2^+ \rightarrow 3_\gamma^+$ transitions which have therefore been assumed to be pure $E2$. The notation $\equiv$ defines the transitions used for normalization in case where an intraband transition was not measured.

For the β band (the left side of Fig. 5), the agreement for the three possible branches is also good. It should be noted at this point that, in plotting the corresponding figure in Ref. 8, the experimental intensity for the $2^+ \rightarrow 4_g^+$ transition was inadvertently omitted from the sum for this branch and the results of the addendum in Ref. 7 were not known. However, the essential conclusion which can be drawn from this figure remains unchanged, namely, the dominance of the branch to the γ band. The right side of Fig. 5 shows the branches from the 0_3^+ band, and the similarity between the decay patterns of the two 0^+ bands is evident both for theory and experiment. However, as mentioned earlier, it is also clear that the ground state branch from the 0_3^+ band is far stronger experimentally than predicted.

For the decays of the second and third 2^+

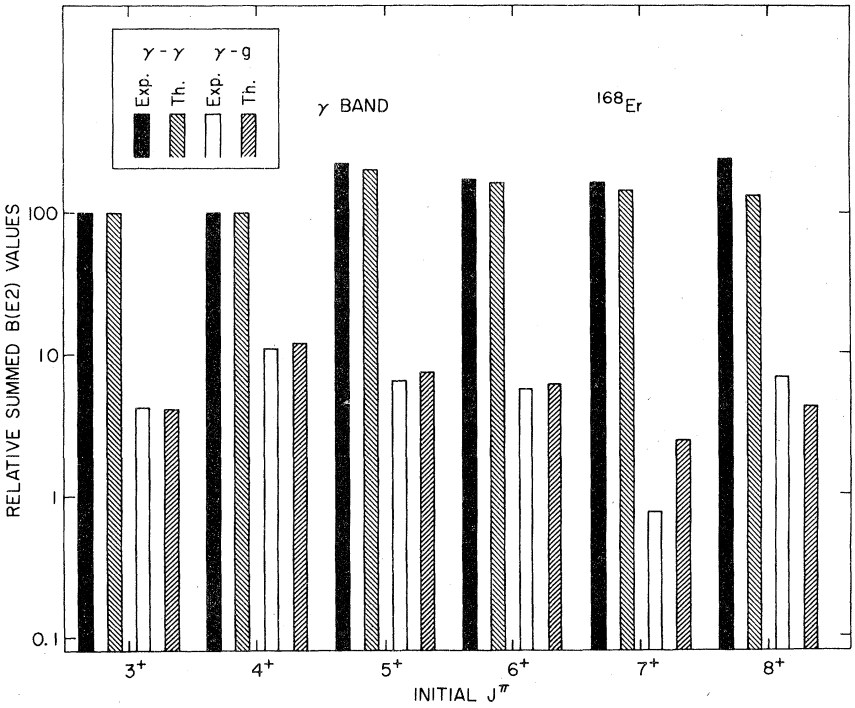

FIG. 4. Comparison of the calculated and experimental summed $B(E2)$ strengths from states in the γ band. For each initial state, the bars represent the sum of all observed or calculated transitions to either the γ band or ground band.

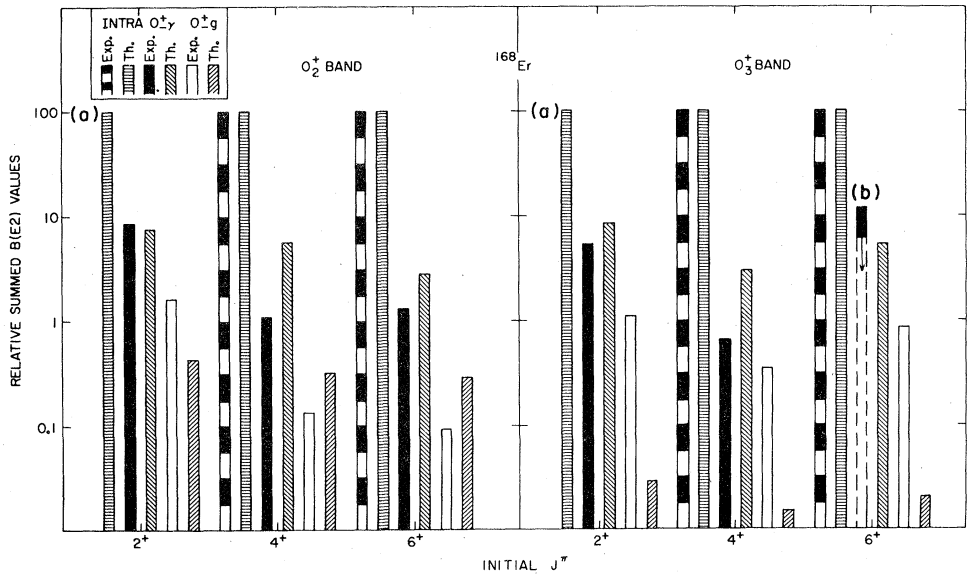

FIG. 5. Comparison of the calculated and experimental summed $B(E2)$ strengths from states in the 0_2^+ and 0_3^+ bands. For each initial state, the bars represent the sum of all observed or calculated transitions to a given final band. The normalization for each case is defined in Tables II and III. The symbol (a) denotes that no experimental information was available for the strength of the intraband transition in these cases. The symbol (b) denotes that the experimental upper limit for this transition has been plotted.

bands, found experimentally at 1848 and 1930 keV, the relatively small amount of data available prohibits the formulation of a detailed comparison, as made for the lower bands. In particular, those transitions that have been observed for the most part have no multipolarity determinations associated with them, or have been measured as predominantly $M1$. The IBA calculations predict that the dominant branches from both these 2^+ bands should be to the first and second excited 0^+ bands followed by the branch to the γ band, while the branch to the ground state band is predicted to be the weakest. Examination of the data[7] shows some indications that these trends are followed, but no detailed conclusions can be drawn.

In considering the overall quality of the IBA predictions for $B(E2)$ values, the specific philosophy behind the calculations presented here should be recalled. The purpose of this study was to reproduce the essential overall features of the observed level scheme in a situation close to the SU(3) limit so that the specific predictions resulting from that symmetry could be compared with experiment. To this end, the parametrization of the Hamiltonian was kept as simple as possible, and there were no free parameters associated with the $E2$ operator. Thus the reproduction of quantitative details such as, for instance, the specific magnitude of deviations from the Alaga rules evidenced by transitions from the γ and β bands are outside the scope of such a treatment. However, the source and magnitude of the perturbations which could give rise to these deviations will be discussed more fully in Sec. V. While these discrepancies in certain details are evident from Tables I—III, the branching ratio data has specifically been presented in bar graph form in Figs. 4 and 5 to emphasize the important features, namely the reproduction of gross intrinsic matrix elements which range over three orders of magnitude. Given this approach, examination of Tables I—III and Figs. 4 and 5 show a very good overall reproduction of the data, but it is also clear that the detailed agreement becomes less precise as the intrinsic excitation energy of the bands increase, the most serious discrepancies involving the ground state branches. These trends may be principally attributable to two complementary effects. Firstly, with increasing excitation energy, the amplitude of admixtures of two quasiparticle and other excitations, outside the IBA basis, is likely to increase; secondly, it can be seen from Tables I—III that the predicted *absolute* strengths of the ground state branches become progressively weaker with increasing bandhead energy. Thus the "purely collective" strength becomes weaker while the noncollective admixtures presumably become larger, and hence, the discrepancies between theory and experiment become greater. While there may certainly be other explanations for specific discrepancies, it seems reasonable that the above effects may contribute to the overall trends observed. It should also be noted that in the description of these very weak transitions, it is possible that higher order terms in both the IBA Hamiltonian and the $E2$ operator may become significant. These considerations also show the necessity, in a more general sense, of considering the absolute magnitude of transition strengths in judging the significance of discrepancies between theory and experiment. This point will become even more apparent in the next section, when the significance of observed $M1$ components is discussed. In the case of $B(E2)$ values, it is interesting to note that the level at which disagreements become apparent is not, as might be naively expected, 1 s.p.u., but rather $\lesssim 0.1$ s.p.u. For instance, the transitions between γ and ground bands are well reproduced and would certainly be thought of as collective, yet their predicted absolute strength is ~ 1 s.p.u. An explanation can be found by considering the microscopic structure of the collective excitations. Since the $E2$ transition strengths between two quasiparticle Nilsson basis states are generally $<< 1$ s.p.u. and since typical amplitudes of component two quasiparticle states in low lying levels are < 1, expected transition rates should be $<< 1$ s.p.u. in the absence of coherence. Thus, resultant strengths of $0.1-1.0$ s.p.u. must result from a *coherent* summation when connecting two low lying composite states and, in fact, represent definite collective enhancements.

Finally, in Tables I—III, the squares of the various effective intrinsic $E2$ matrix elements have been listed. The constancy of these values for a set of transitions to a given final band reflects the closeness of the IBA predictions to those expected from the application of the Alaga rules in the geometrical description.

IV. $M1$ TRANSITIONS

It was mentioned in the previous section that one interesting experimental feature in the decay of the two excited 0^+ bands is the occurrence of a sequence of $I \rightarrow I$ transitions to the ground state band whose multipolarities have been determined as

essentially pure $M1$, and that such transitions might throw some doubt on the validity of a collective interpretation for these bands. It is thus worthwhile to consider the significance of these transitions in more detail.

The occurrence in deformed nuclei of transitions from the γ band with significant $M1$ components has been recognized for some time. The usual explanations for such components have involved the assumption of a small departure from collectivity in terms of either a small difference between the g factors of the ground and gamma bands, or small admixtures of unobserved $K^\pi = 1^+$ bands. However, it has recently been shown[15] that the constancy and size of the $M1$ admixtures in the intraband transitions in the gamma bands of deformed rare-earth nuclei do not support this type of interpretation, but instead suggest that a collective effect is responsible. It was demonstrated that the theory of Greiner,[17] which deduces these $M1$ admixtures from a proposed difference in deformation of the proton and neutron cores, meets with considerable success. This comparison included, in fact, results for the intraband γ band transitions in ^{168}Er.

In assessing the importance of $M1$ transitions from the 0^+ bands, it is thus useful to consider the strength of these transitions in absolute terms and to compare them with their counterparts in the gamma band. To this end, the empirical absolute magnitudes (in single particle units) of several $M1$ transitions in the gamma and 0^+ bands have been calculated. These estimates have been extracted as follows: For each case the estimate has been based on the value of the branching ratio between the $M1$ transition of interest and an *intra*band $E2$ transition. The Weisskopf single particle estimate[11] for $T(\sigma\lambda;0\rightarrow\lambda)$ was used to calculate each branching ratio, and the IBA results were used to predict the strength of the collective $E2$ transition in each case. The experimental value for the branching ratio then yields an estimate of the single particle strength of the $M1$ transition. The steps in this procedure are listed in Tables IV and V, where the first column in each case gives the $M1$ and $E2$ transitions in the branching ratio, the second and third columns list the experimental and Weisskopf values for this branching ratio, and the fourth column lists the calculated strength of the $E2$ transitions.

The estimated absolute $M1$ strengths for transitions from the γ band are listed in the final column of Table IV. It can be seen that the constancy of the strengths of the intraband $M1$ components is confirmed in absolute terms, and is shown to be at the level of 8×10^{-4}s.p.u. It is also worth noting that the two interband transitions which could be es-

TABLE IV. Estimate of $M1$ s.p. strengths for some transitions from the gamma band of ^{168}Er.

Transitions $M1/E2$	$T(M1)/T(E2)$ Exp.[a]	$T(M1)/T(E2)$ s.p. estimate[b]	Calculated intraband $B(E2)$ (s.p.u.)	$B(M1)$ (s.p.u.)
$\frac{3_1^+\rightarrow 2_2^+}{3_1^+\rightarrow 2_2^+}$	0.49	5.0×10^4	66.2	6.5×10^{-4}
$\frac{5_1^+\rightarrow 4_2^+}{5_1^+\rightarrow 3_1^+}$	0.03	0.10×10^4	35.0	1.1×10^{-3}
$\frac{6_2^+\rightarrow 5_1^+}{6_2^+\rightarrow 4_2^+}$	0.01	0.06×10^4	42.8	7.2×10^{-4}
$\frac{7_1^+\rightarrow 6_1^+}{7_1^+\rightarrow 5_1^+}$	0.82	6.3×10^4	47.2	6.2×10^{-4}
$\frac{7_1^+\rightarrow 8_1^+}{7_1^+\rightarrow 5_1^+}$	0.35	1.2×10^4	47.2	1.4×10^{-3}

[a] The experimental ratios have been obtained from the data of Refs. 7 and 15.
[b] The single particle estimates have been calculated using the Weisskopf estimate of $T(\sigma\lambda;0\rightarrow\lambda)$ for each member of the $M1/E2$ branching ratio listed in the first column.

TABLE V. Estimate of $M1$ s.p. strengths for some transitions from the excited 0^+ bands of ^{168}Er.

Transitions[a] $M1/M2$	$T(M1)/T(E2)$ Exp.[b]	$T(M1)/T(E2)$ s.p. estimate[c]	Calculated intraband $B(E2)$ (s.p.u.)	$B(M1)$ (s.p.u.)
$\frac{4^{+'}\rightarrow 4_1^+}{4^{+'}\rightarrow 2^{+'}}$	11.2	9.5×10^6	47.5	5.7×10^{-5}
$\frac{6^{+'}\rightarrow 6_1^+}{6^{+'}\rightarrow 4^{+'}}$	3.8	0.9×10^6	51.4	2.2×10^{-4}
$\frac{4^{+''}\rightarrow 4_1^+}{4^{+''}\rightarrow 2^{+''}}$	132.4	6.6×10^6	45.5	9.2×10^{-4}
$\frac{6^{+''}\rightarrow 6_1^+}{6^{+''}\rightarrow 4^{+''}}$	23.9	0.8×10^6	49.0	1.5×10^{-3}

[a] The notation $I^{+'}$, $I^{+''}$ refers to states in the 0_2^+ and 0_3^+ bands, respectively.
[b] The experimental ratios have been obtained from the data of Ref. 7.
[c] The single estimates have been calculated using the Weisskopf estimate of $T(\sigma\lambda;0\rightarrow\lambda)$ for each member of the $M1/E2$ branching ratio listed in the first column.

timated show identical $M1$ strengths. Given their constancy, the small size of these $M1$ amplitudes indeed supports a collective origin.

Turning now to the 0^+ bands, Table V indicates that the strengths of the pure $M1$ $I\rightarrow I$ transitions to the ground band are actually of the same order of magnitude or less than those in the γ band. Thus these transitions do not indicate any significant departure from collectivity but rather arise because of the weakness of the competing $E2$ modes which, as can be seen in Tables II and III, are predicted to lie at a level of < 0.1 s.p.u. It should be noted that $M1$ matrix elements have also been extracted for the $I\rightarrow I$ transitions between the 0_2^+ and ground bands of ^{174}Hf,[3] again indicating a strength of $\sim 10^{-4}$ s.p.u. in this case.

One further remark might be made concerning the preceding analysis. Since the rigorous collective model forbids $M1$ transitions in even-even nuclei, the small absolute $M1$ strengths extracted in the preceding analysis show that the perturbations to this concept are indeed very small. Conversely, however, the analysis also indicates that the use of *collectivity* as an argument to justify the *assumption* of pure $E2$ transitions in deformed even-even nuclei is dangerous, since $B(M1)$ values of only $10^{-4}-10^{-5}$ s.p.u. can still result in significant, or dominant, $M1$ components.

V. COMPARISON WITH A GEOMETRICAL DESCRIPTION

It is hardly surprising that the results of an IBA calculation for a well deformed nucleus such as ^{168}Er are similar to those which would be obtained from the geometrical model, given the proven success of the latter for this class of nuclei. It is thus of considerable interest to study the relationship between the two descriptions both to understand the IBA predictions in a familiar framework and to highlight the differences between the two approaches. In this section, therefore, the data for the first three positive parity bands of ^{168}Er have been analyzed in terms of a band-mixing approach and an attempt has been made to compare and contrast the results and philosophy of such a treatment with those of the IBA calculations presented previously.

It was mentioned earlier that the IBA wave functions effectively incorporate finite admixtures between different (pure K) bands, even in the SU(3) limit. It was also pointed out that one of the fundamental characteristics of this limit was the prediction of a dominant $\beta\rightarrow\gamma$ $E2$ branch, in contrast to the selection rule of the geometrical model which would forbid $n_\beta = 1\rightarrow n_\gamma = 1$ transitions. The question therefore arises as to the mechanism producing this dominance in the IBA, expressed in

the framework of a geometrical description. The matrix elements connecting β and γ bands in the IBA, even in the SU(3) limit, contain two classes of terms[9] of different origin. One is a $\Delta K = 0$ term arising from finite, albeit small, admixtures of $K = 0$ components in the γ band which arise from the transformation between Elliott and Vergados bases and from the requirements of orthogonality. This term is directly analogous to that producing $\beta \rightarrow \gamma$ transitions in the geometrical description via $\beta - \gamma$ band mixing (see below), except that its strength goes to zero in the infinite dimensional limit. The second type of term is a direct $\Delta K = 2$ term which has no precise analog in the geometrical description although it can be introduced *ad hoc*. This term does not go to zero in the infinite dimensional limit and, indeed, is the one responsible for the IBA prediction of relative $\beta \rightarrow \gamma$ transition strengths that agree with the Alaga rules in that limit.

It has long been recognized that the predictions of the geometrical model for relative interband transition strengths (i.e., Alaga rules) are not precisely followed and it has become standard practice to introduce perturbations, in the form of explicit band mixing, to account for these deviations. For example, extensive literature (see, for example, Refs. 3, 18, and 19) supports the conclusion that significant improvement in the predictions of the geometrical model for $\gamma \rightarrow g$ transitions is obtained by the introduction of two band $\gamma - g$ mixing, usually specified in terms of a mixing parameter z_γ. Similar improvements, while less extensively documented due to lack of empirical information, are obtained for the $\beta \rightarrow g$ transitions by the use of a z_β parameter to reflect $\beta - g$ mixing. Finally, fine tuning of some of the predicted $E2$ $\beta \rightarrow g$ and $\gamma \rightarrow g$ branching ratios has sometimes been obtained with the inclusion of direct $\beta - \gamma$ mixing in a three-band mixing calculation.

It is clear that direct $\beta - \gamma$ mixing will also lead to $\beta \rightarrow \gamma$ transitions via amplitudes leading to effective intraband matrix elements. However, while this implication of the often introduced $\beta - \gamma$ mixing is inescapable, it has not been generally recognized nor studied, again primarily due to the lack of data. The recent results for ^{168}Er, however, provide an ideal opportunity to test whether explicit $\beta - \gamma$ mixing can account for the observed dominance of $\beta \rightarrow \gamma$ over $\beta \rightarrow g$ transitions and whether the calculated relative $\beta \rightarrow \gamma$ $B(E2)$ values agree with experiment.

To this end, we have performed three band mixing calculations according to the usual formalism. For $\gamma \rightarrow g$ and $\beta \rightarrow g$ transitions, the formulas are given in detail in Ref. 18 and the expressions for specific transitions are tabulated. However, for $\beta \rightarrow \gamma$ transitions the required expression has not yet been presented. It has been derived by Riedinger[20] and its structure is informative. Assuming that the direct $\Delta K = 2$ $\beta \rightarrow \gamma$ intrinsic matrix element vanishes, one has

$$B(E2{:}I_\gamma \rightarrow I'_\beta) = \frac{2Q_{00}{}^2 Q_\gamma{}^2}{Q_\beta{}^2} \left[\frac{1}{\sqrt{6}} z_{\beta\gamma} [f_2(I'_\beta)\langle I_\gamma 220 \,|\, I'_\beta 2\rangle - f_2(I_\gamma)\langle I_\gamma 200 \,|\, I'_\beta 0\rangle] + \frac{1}{\sqrt{24}} z_\gamma \frac{Q_\beta{}^2}{Q_{00}{}^2} f_2(I_\gamma)\langle I_\gamma 200 \,|\, I'_\beta 0\rangle + z_\beta \frac{Q_\beta{}^2}{Q_{00}{}^2} f_0(I'_\beta)\langle I_\gamma 22 - 2 \,|\, I'_\beta 0\rangle \right]^2 , \tag{8}$$

where $f_0(I) = I(I+1)$,
$f_2(I) = [(I-1)I(I+1)(I+2)]^{1/2}$, and the intrinsic $E2$ matrix elements Q are defined in terms of the $B(E2)$ values by the equations

$$B(E2{:}0_g \rightarrow 2_g) = Q_{00}{}^2 , \tag{9}$$

$$B(E2{:}0_g \rightarrow 2_\gamma) = 2Q_\gamma{}^2[1 - z_\gamma + 2z_{\beta\gamma}]^2 , \tag{10}$$

$$B(E2{:}0_g \rightarrow 2_\beta) = Q_\beta{}^2[1 - 6z_\beta - 4z_{\beta\gamma}Q_\gamma{}^2/Q_\beta{}^2]^2 . \tag{11}$$

The constants Q_β, Q_γ, and Q_{00} may be deduced from measured $B(E2)$ values, and an assumed set of z parameters.

The first term in the bracket of Eq. (8) arises from direct mixing of the β and γ bands. The last two arise from second order mixing via the ground band. Noting that Q_{00} is an intraband matrix element and that Q_β is the relatively weak $\beta \rightarrow g$ interband element, it is evident that the last two terms are much smaller than the first. Neglecting these for the moment, one has

$$B(E2{:}I_\gamma \rightarrow I_\beta) = \frac{Q_{00}{}^2 Q_\gamma{}^2}{3Q_\beta{}^2} z_{\beta\gamma}{}^2 F^2(I_\gamma, I'_\beta) , \tag{12}$$

where $F(I_\gamma, I'_\beta)$ is evident by comparison of

Eqs. (8) and (12).

Thus, one has the surprising result that the *relative* sizes of the various $\gamma \rightarrow \beta$ $B(E2)$ values are *independent* of $z_{\beta\gamma}$ while scaling approximately as $z_{\beta\gamma}^2$. This independence is in striking contrast to the strong dependence on z_γ and z_β of the $\gamma \rightarrow g$ and $\beta \rightarrow g$ transitions where the mixing term is a *correction* to a nonzero *intrinsic* matrix element. Thus, the predicted $\beta \rightarrow \gamma$ $E2$ branching ratios are independent of possible uncertainties in the adopted value of $z_{\beta\gamma}$. For the sake of rigor in the calculations below, the full Eq. (8) is used rather than the approximation of Eq. (12) but in all cases the differences are negligible.

In performing a three band mixing calculation, there are six parameters that must be fixed. Two of these, $B(E2{:}0_g^+ \rightarrow 2_g^+)$ and $B(E2{:}0_g^+ \rightarrow 2_\gamma^+)$, were taken from experiment and, as with the IBA calculations, these ensure reasonably accurate intraband and interband $E2$ matrix elements for decays from the γ band. Realizing that z_γ has virtually no effect on $\beta \rightarrow \gamma$ transitions, and that $z_{\beta\gamma}$ has a much smaller effect on $\gamma \rightarrow g$ than on $\beta \rightarrow g$ transitions (see Table III of Ref. 18), z_γ parameters for each $\gamma \rightarrow g$ branching ratio were extracted by requiring agreement of a two band mixing calculation with the data. The adopted value of $z_\gamma = 0.038$ provides a reasonable reproduction of the overall set of $\gamma \rightarrow g$ branching ratios. It is clear from Eqs. (11) and (12) that the strength of $\beta \rightarrow \gamma$ transitions depends approximately on the quantity $z_{\beta\gamma}^2 / B(E2{:}0_g^+ \rightarrow 2_\beta^+)$. Reference to the formulas of Ref. 18 shows that the $\beta \rightarrow g$ branching ratios depend on $z_{\beta\gamma}/B(E2{:}0_g^+ \rightarrow 2_\beta^+)$ as well as z_β. Note that this $B(E2)$ value is unknown empirically. Thus the fitting procedure consisted of varying $z_{\beta\gamma}$

TABLE VI. Comparison of experimental and theoretical $B(E2)$ values for the 0_2^+ band in ^{168}Er.

J_i^π	J_f^π, K[a]	Calculated absolute[b] $B(E2;I^i \rightarrow I_f)$ (s.p.u.)	Relative $B(E2{:}I_i \rightarrow I_f)$[c] BM	Exp.	IBA
2^+	$0^+,0$	0.007	0.02	0.005	0.002
	$4^+,0$	0.04	0.10	0.03	0.008
	$2^+,2$	0.11	0.27	0.10	0.06
	$3^+,2$	0.05	0.12	$\equiv 0.12$	$\equiv 0.12$
	$0^+,0'$	42.85	100.0		
4^+	$2^+,0$	0.01	0.02	0.02	0.09
	$6^+,0$	0.07	0.11	0.11	0.23
	$2^+,2$	0.06	0.10	0.03	0.04
	$3^+,2$	0.40	0.65	0.35	0.63
	$4^+,2$	0.13	0.21	0.52	2.2
	$5^+,2$	0.37	0.61	0.19	2.8
	$2^+,0'$	61.28	100.0	100.0	100.0
6^+	$4^+,0$	0.02	0.04	0.02	0.07
	$8^+,0$	0.12	0.18	0.07	0.21
	$4^+,2$	0.35	0.51	0.11	0.09
	$5^+,2$	0.96	1.42	0.32	0.73
	$6^+,2$	0.13	0.19	0.93	2.0
	$4^+,0'$	67.49	100.0	100.0	100.0

[a] The notation $0'$ refers to the 0_2^+ band.

[b] $B(E2)$ values, calculated in the band-mixing framework, using 1 s.p.u. $= 0.0269\ e^2b^2$. The intraband transitions from the 4^+ and 6^+ levels were calculated assuming the simple rotational limit dependence on Clebsch-Gordan coefficients. This neglects the small ($\lesssim 2\%$) correction on these transitions as well due to the mixing.

[c] The column BM gives the relative $B(E2)$ values calculated with the band-mixing formalism discussed in the text [see Eq. (8)]. The IBA entries are the same as in Table II except that, for convenience of comparison here, the normalization for the 2^+ initial state is changed to be the same as in the BM calculation. The experimental transitions are corrected for $M1$ admixtures and are normalized to an intraband transition except for the 2^+ level, where none was observed and the $2^+ \rightarrow 3^+$ transition was used instead.

to obtain the desired $\beta \rightarrow \gamma$ dominance while at the same time varying z_β and $B(E2{:}0_g^+ \rightarrow 2_\beta^+)$ to obtain reasonable $\beta \rightarrow g$ branching ratios and to set the absolute scale of the $\beta \rightarrow g$ $B(E2)$ values by forcing the calculated and experimental values to agree for the $4_\beta^+ \rightarrow 6_g^+$ transition. From these procedures, the values $z_\beta = 0.038$, $z_{\beta\gamma} = -0.00086$, and $B(E2{:}0_g^+ \rightarrow 2_\beta^+) = 0.0010\ e^2b^2$ were obtained. Different sets of z_β and $B(E2;0_g^+ \rightarrow 2_\beta^+)$ parameters would primarily affect only the $\beta \rightarrow g$ branching ratios.

The essential results are the following: The calculations excellently reproduce the $\gamma \rightarrow g$ $B(E2)$ values, the largest disagreements being typically only 20–30%. The detailed results for transitions from the β band are given in Table VI and it can be seen that the $\beta \rightarrow g$ $B(E2)$ values are reasonably well accounted for.

Of course, given the fitting procedure described earlier, the average $\beta \rightarrow \gamma / \beta \rightarrow g$ branching ratio is reproduced. It is interesting, and at first glance surprising, to note that this $\beta \rightarrow \gamma$ dominance is obtained with a very small $z_{\beta\gamma}$ parameter value and one that is fully consistent with, and indeed perhaps smaller than, values typically extracted in rare earth nuclei in the past. The clear implication, therefore, which matches that of the IBA, is that one now expects a *general $\beta \rightarrow \gamma$ dominance in most deformed rare earth nuclei.* In retrospect it is easy to see why this is so. It results from the strength of the intrinsic intraband $E2$ matrix element, which is admixed by the β-γ band mixing, over the $\beta \rightarrow g$ interband matrix element.

Lastly, in comparing the band-mixing calculations with the data one notes that although the $\beta \rightarrow \gamma$ dominance is reproduced (or, more precisely, is *defined* to be reproduced and the required $z_{\beta\gamma}$ is thereby extracted), the detailed relative $\beta \rightarrow \gamma$ $B(E2)$ values are not in good agreement with the data. It is worth recalling that these are essentially invariant [see Eq. (12)] and, therefore, in the context of this model cannot be improved.

Thus, to summarize at this stage, the empirical $\beta \rightarrow \gamma$ dominance can be reproduced both in the IBA basis, where it results naturally from the underlying SU(3) symmetry, and in the band-mixing formalism, using a $z_{\beta\gamma}$ parameter of the same order as deduced from previous studies of $\gamma \rightarrow g$ and $\beta \rightarrow g$ transitions in rare earth nuclei. The quality of the overall reproduction of branching ratios from the β band is comparable in both models and in fair agreement with the data, as can be seen in Table VI. The essential difference between the two descriptions lies in the *mechanism* by which the $\beta \rightarrow \gamma$ dominance is reproduced. In the geometrical description it results purely from mixing between β and γ bands; in the IBA it comes primarily from an *intrinsic $\beta \rightarrow \gamma$* matrix element.

It is important, therefore, to enquire whether the *experimental* information can yield the source of the dominance. To this end, following a suggestion of Ref. 12, the data for the first three bands have been analyzed using the first order I-dependent intensity relations described in Ref. 3. This technique corresponds to treating the deviations from the leading order (Alaga) intensity rules for transitions between any two bands as resulting simply from mixing between these two bands and can be analyzed in the form of a graphical technique known as a Mikhailov plot.[21] The transition strengths are given by

$$B(E2;I_1K_1 \rightarrow I_2K_2) = 2\langle I_1K_1 22 \,|\, I_2K_2\rangle^2 \{ M_1 + M_2[I_2(I_2+1) - I_1(I_1+1)] \}^2 , \tag{13}$$

for $\Delta K = 2$ transitions, where

$$K_2 = K_1 + 2 ,$$

$$M_1 = \langle K_2 \,|\, M(E2) \,|\, K_1 \rangle - 4(K_1+1)M_2 ,$$

$$M_2 = \left[\frac{15}{8\pi} \right]^{1/2} eQ_0\epsilon_2 .$$

Here, ϵ_2 is the spin independent amplitude describing the admixture of the two bands and Q_0 is the intrinsic quadrupole moment, calculated from the experimental value of $B(E2;0_g^+ \rightarrow 2_g^+)$ to be 7.61 b for ^{168}Er. Thus, the square root of Eq. (13) can be represented by a straight line by plotting $[B(E2;I_1K_1 \rightarrow I_2K_2)]^{1/2} / \sqrt{2}\langle I_1K_1 22 \,|\, I_2K_2\rangle$ against $I_2(I_2+1) - I_1(I_1+1)$. The slope M_2 and intercept M_1 then yield the mixing and intrinsic $E2$ matrix elements, respectively. Note that this approach is exactly equivalent to that previously described in the two band mixing case, where z_β and $z_{\beta\gamma}$ are zero. Then z_γ can be expressed as

$$z_\gamma = \frac{-2M_2}{M_1 + 4M_2} . \tag{14}$$

For $\Delta K = 0$ transitions, the equivalent expressions become

$$B(E2;I_1K \rightarrow I_2K) = \langle I_1K20 \mid I_2K\rangle^2\{ M_1 + M_2[I_2(I_2+1) - I_1(I_1+1]\}^2 ,$$
$$M_1 = \langle K \mid M(E2) \mid K\rangle , \tag{15}$$
$$M_2 = \left[\frac{5}{16\pi}\right]^{1/2} eQ_0\epsilon_0 .$$

To the extent that three band mixing effects are important, this approach will be inadequate. As pointed out before, these effects are relatively unimportant for $\gamma \rightarrow g$ transitions, and they are negligible for $\beta \rightarrow \gamma$ transitions. The $\beta \rightarrow g$ transitions, however, can be strongly perturbed by three band mixing effects. The use of the two band approach, which gives the leading order I-dependent expressions, has, however, two advantages. Firstly, the IBA results can be simply studied by this technique, and the effective coupling and intrinsic matrix elements extracted. This is true only to the extent that the IBA intensities form a straight line when plotted in the format of Eqs. (13) or (15). Secondly, the analysis of the experimental $\beta \rightarrow \gamma$ transitions by this method will automatically yield an intercept corresponding to the *ad hoc introduction of an intrinsic* $\beta \rightarrow \gamma$ *matrix element* into the geometrical description. Again, if the data points can be fitted by a straight line, such an analysis will provide an empirical value for this matrix element, and thus distinguish which mechanism is responsible for the observed $\beta \rightarrow \gamma$ dominance.

Thus, both the IBA results and the experimental data for the $\gamma \rightarrow g$, $\beta \rightarrow \gamma$, and $\beta \rightarrow g$ transitions have been analyzed in the form of Mikhailov plots, and the results for the first case are shown in Fig. 6. It is evident from this figure that the IBA results can be reasonably well approximated by a straight line, and this is true for the other cases also. The results of these analyses are presented in Table VII, where the extracted values of M_1 and M_2 are listed, as well as the implied values of the intrinsic $E2$ matrix element. In addition, the implied coupling matrix element $h_{\Delta K}$ can be extracted from the mixing amplitude $\epsilon_{\Delta K}$ as follows:

$$h_{\Delta k} = \epsilon_{\Delta k}[E(K_2) - E(K_1)] . \tag{16}$$

A study of Table VII provides answers to several crucial questions. Consider first the intrinsic $E2$ matrix elements. The experimental data for $\beta \rightarrow \gamma$ transitions can be fitted with a straight line ($\chi^2 = 0.5$), and thus can be used to test for an intrinsic matrix element. As shown in Eq. (13), the condition for a zero $\beta \rightarrow \gamma$ $E2$ element, corresponding to a $\beta \rightarrow \gamma$ dominance arising from $\beta - \gamma$ band mixing alone, is given by

$$M_1 = -4M_2 , \tag{17}$$

and it is evident that the data simply do not permit such a conclusion and, in fact, give direct evidence for a nonzero intrinsic $E2$ matrix element of 0.094(7) e b. This empirical result shows that the mechanism for the $\beta \rightarrow \gamma$ dominance is exactly that predicted by the IBA, and the value of the predicted intrinsic element is within roughly a factor of 2 of the data. For $\beta \rightarrow g$ transitions the IBA intrinsic matrix element is again roughly a factor of 2 too high, so that the ratio of $\beta \rightarrow \gamma/\beta \rightarrow g$ matrix elements is very similar in the data and the IBA. The $\gamma \rightarrow g$ $E2$ matrix element was, of course, used to fix the constants of the $E2$ operator in the IBA calculation, and hence, the agreement with experi-

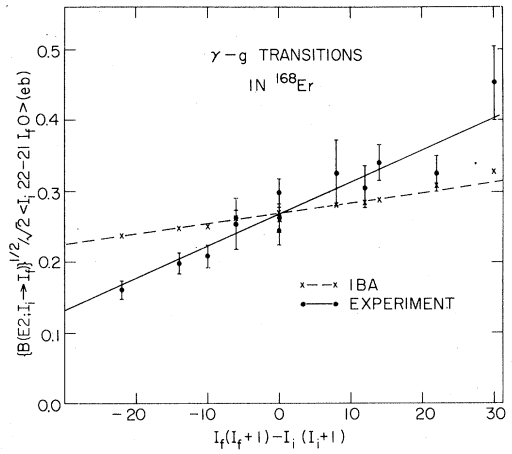

FIG. 6. Mikhailov plots for transitions between gamma and ground bands in ^{168}Er. The dashed line represents a fit to the values predicted by the IBA calculation. The solid line represents a linear least squares fit to the experimental data, using results for all transitions originating from states up to and including the 6^+ member of the gamma band. The absolute scale was determined from the known value of $B(E2;0_1^+ \rightarrow 2_1^+)$ for transitions from the 2^+ state, and from the predicted absolute strength of the *intra*band transitions from the higher states. Note that by the definitions of Eq. (13), $I_2 = I_i$, and $I_1 = I_f$, and hence, the positive slopes of the two lines imply negative values of M_2.

TABLE VII. Comparison of values of intrinsic and coupling matrix elements extracted from Mikhailov plots of the experimental data and the IBA predictions for ^{168}Er.

	Initial and final bands					
	$2_1^+ \rightarrow 0_1^+$		$0_2^+ \rightarrow 0_1^+$		$0_2^+ \rightarrow 2_1^+$	
	Exp[a]	IBA	Exp[b]	IBA	Exp[b]	IBA
M_1 (e b)	0.268(6)	0.269	0.039(2)	0.069	0.108(7)	0.201
M_2 (e b)	−0.0045(5)	−0.0014	−0.0006(1)	−0.0005	−0.0036(6)	0.0015
$\langle K_i \mid M(E2) \mid K_f \rangle$ (e b)	0.250(6)	0.263	0.039(2)	0.069	0.094(7)	0.207
$\langle K_i \mid h_{\Delta K} \mid K_f \rangle$ (keV)	−0.57(6)	−0.181	−0.29(5)	−0.27	0.28(5)	−0.11

[a] The experimental values are extracted from a linear least squares fit using results for all transitions originating from states up to and including the 6^+ member of the gamma band. Transitions from the two higher levels were not included because of uncertainties in the $M1$ components. The absolute scale was determined from the known value of $B(E2;0_1^+ \rightarrow 2_2^+)$ for the transitions from the 2^+ state, and from the predicted absolute strength of the *intra*-band transitions from the higher states.

[b] All transitions from the 4^+ and 6^+ members of the 0_2^+ band were included in the linear least squares fit, the absolute normalization being based on the absolute predicted strength for the *intra*band transitions in each case. For the $0_2^+ \rightarrow 2_1^+$ case, the strength of the $2^+ \rightarrow 3^+$ transitions, *relative* to the $2^+ \rightarrow 2^+$ strength, was included in the fit to the experimental data.

ment is to be expected in this case.

Turning now to the values for the slopes of the experimental and IBA lines, we observe that, while the empirical value for the $\beta \rightarrow g$ transitions is well reproduced, the $\gamma \rightarrow g$ and $\beta \rightarrow \gamma$ values deviate from the data by factors of ~ 3. However, the significance of these deviations can be judged from the corresponding values of the coupling matrix elements, $h_{\Delta K}$. It can then be seen that they imply, at worst, differences of $\lesssim 0.4$ keV in the predicted and experimental coupling matrix elements between the bands. It is important to understand this point and its implications. Inspection of Table I, for example, shows that while the IBA provides an excellent overall description of the relative $B(E2)$ values there are, nevertheless, discrepancies of factors of 2 for certain interband transitions. These seemingly large differences arise directly from differences of ~ 0.4 keV between the empirical and effective IBA mixing matrix elements because the resultant admixed amplitudes ($\sim 10^{-3}$) correspond to those for *intra*band transitions and thus their effects are enormously *magnified*. Given the philosophy and consequent simple parametrization behind the IBA calculations presented here, such differences are neither surprising nor disturbing.

The conclusion concerning the application of the IBA to the β, γ, and ground bands of ^{168}Er is thus clear. The calculations have reproduced the absolute intrinsic $E2$ matrix elements, which range over three orders of magnitude experimentally, to within a factor of 2 or better. The intrinsic coupling matrix elements between bands have been reproduced to within 0.4 keV. In addition, of course, the complete sequence of experimental bands below the pairing gap has been obtained with the exception of the $K^\pi = 3^+$ and 4^+ bands discussed previously. This complete description of the collective states resulted from a total of five parameters, four of which were fixed from simple prescriptions and only one of which was allowed to vary freely.

The 0_3^+ band deserves particular attention. This band cannot, of course, be included in the three band mixing formalism presented at the beginning of this section, while the small amount of data which exists for the branch to the gamma band, for instance, cannot be represented by the I-dependent intensity rules. Inspection of Table III, however, shows that in the case of transitions from the 4^+ state, where an absolute normalization is available, the branch to the gamma band is overestimated in two cases by the IBA, each by a factor of ~ 5, while in one case it is underestimated by a factor of ~ 2. Thus this information points to a predicted

matrix element which is within a factor of 2 of the data. The intensities to the ground band are overestimated by an order of magnitude, and the significance and possible sources of this discrepancy have already been discussed in Sec. III.

In considering the analog of this band in the geometrical model, the natural choice would be an $n_\gamma = 2$ assignment. While such a correspondence may be correct in part, it should be noted that in the geometrical description, the $B(E2)$ values for $n_\gamma = 2 \rightarrow n_\gamma = 1$ transitions would be expected to equal those for $n_\gamma = 1 \rightarrow n_\gamma = 0$ transitions. Inspection of the squares of the intrinsic matrix elements extracted from the IBA results for the corresponding transitions, given in column 4 of Tables I and III, shows that in the IBA, the intrinsic $E2$ matrix element between the 0_3^+ band and gamma band, is actually *half* that between the gamma and ground bands. Thus it would appear that the correspondence between the IBA and geometrical descriptions for this and possibly higher bands is no longer simple.

It could be suggested that, since application of the first order I-dependent intensity rules, or band-mixing formalism, gives comparable or better results for the detailed relative $E2$ intensities, such a technique represents a preferable description of the nucleus. Such considerations should be tempered by the realization that this formalism involves the *separate* parametrization of the relative transition strengths between *each pair of bands,* in the form of an intrinsic $E2$ matrix element and a mixing matrix element. Thus, two parameters must be introduced for each pair of bands. In addition, for a complete description of the level scheme, the bandhead energies and inertial constants must be parametrized separately. Complete multiparameter calculations along these lines have indeed been performed in the past,[22] and, not surprisingly, show excellent agreement with the data. However, while such an approach is certainly valuable and instructive, it corresponds effectively to *extracting* the complete set of parameters from the data. In contrast, the IBA aims at *predicting* the same set of physical quantities from a simple treatment of a Hamiltonian and operator which are equally applicable both in neighboring nuclei and in those with widely different structure.

VI. SUMMARY AND CONCLUSIONS

The calculation described above represents the most detailed test to date of the IBA in the region of well deformed nuclei. The overall agreement with the data is impressive, both in terms of the correct prediction of the complete set of positive parity states below the pairing gap, and the reproduction of the intrinsic $E2$ matrix elements, both interband and intraband, which range over three orders of magnitude experimentally. In judging the quality of this agreement, it should be emphasized again that the complete set of levels and branching ratios stem from the use of only one free parameter, the other four constants in the Hamiltonian and $E2$ operator having been fixed from simple prescriptions.

The prediction of absolute $B(E2)$ values allowed the significance of disagreements between theory and experiment to be judged, and it has thus been shown that in certain cases relatively small perturbations would be sufficient to account for observed discrepancies. Similar conclusions apply to the observed $M1$ components in the decay scheme, where the absolute strengths have been estimated to lie in the range of $10^{-3}-10^{-5}$ s.p.u. The additional fact of the constancy of these small absolute $M1$ strengths for the intraband transitions in the gamma band supports the concept of an essentially collective origin.

Undoubtedly, the most crucial result of this study is the prediction of the dominance of the gamma decay branch from the β to the γ band, over that to the ground band, which is in agreement with the data. While it has been shown that such a dominance can be reproduced in the Bohr-Mottelson description for a particular nucleus by the explicit introduction of $\beta-\gamma$ band mixing, in the framework of the IBA, the natural appearance of both a direct $\Delta K = 2$ intrinsic matrix element and the specific band admixtures which give rise to this feature represents a fundamental characteristic arising from the underlying SU(3) symmetry of the model basis and thus represents *a global prediction for all deformed nuclei.* The dominance of $\beta \rightarrow \gamma$ transitions over $\beta \rightarrow g$ and, indeed, the sizes of these relative to the intraband transitions, while confirmed and established in more detail by the most recent study,[7] are already implicit in a comparison of the earlier work of Michaelis *et al.*[23] and Koch.[24] It is certainly possible, and indeed seems likely, that the dominance of the $\beta \rightarrow \gamma$ branch represents a general characteristic of deformed nuclei which has not yet been recognized experimentally, although existing results from studies of ^{158}Gd and ^{172}Yb also demonstrate this dominance.[22,25] The consistent occurrence of this feature

throughout the region of deformed nuclei would lend considerable support to the utility of the IBA Hamiltonian in providing an apt underlying basis for the description of intrinsic collective excitations in deformed nuclei.

Given the very simple parametrization chosen for the model Hamiltonian, it is hardly surprising that discrepancies appear in the detailed comparison of relative branching ratios between particular pairs of bands. Nevertheless, the analysis of Sec. V indicates that these discrepancies result from differences of only a few tenths of a keV in the predicted and experimental coupling matrix elements between the bands. Such disagreements might be partially rectified by "fine tuning" the parameters of the Hamiltonian and/or by adding perturbations. For instance, a reduction in the pairing term will lead to a negative value for the $\beta - \gamma$ coupling matrix element, in better agreement with the data. However, to obtain near perfect agreement in all cases, it would probably be necessary to introduce higher order terms into both the Hamiltonian and the $E2$ operator. There is an analogy here with the approach used in conventional models. The simplest geometrical model gives predictions of rotational bands with constant moment of inertia, harmonic vibrations, and transition intensities obeying the Alaga rules. Deviations from this simple picture are introduced via perturbations and higher order terms in both the Hamiltonian , to describe, for instance, anharmonicities in the location of multiphonon excitations and changes in the moment of inertia, or in the operator; these lead to the I-dependent intensity rules of Eqs. (13) and (15). While the IBA description presented here already incorporates, to some extent, many of these higher order effects, and in addition, of course, yields automatically a large number of quantities which have to be parametrized separately in the geometrical model (energies, intrinsic matrix elements, etc.), it is certainly probable that analogous higher order terms must be included in this IBA formalism to explain the detailed discrepancies which still remain.

To conclude, it should be emphasized once again that while a comparison of the IBA and geometrical descriptions is extremely useful in terms of understanding the successes and failures of the former in a familiar framework, a comparison of the relative quality or usefulness of the two descriptions can only be made if the different philosophies behind each approach are understood. The geometrical model as used here involves a formalism applicable specifically to deformed nuclei, which allows the *extraction* of all the parameters necessary to describe a given nucleus. The IBA uses a Hamiltonian which is applicable across a wide range of nuclei, and which for a certain combination of terms, provides a *prediction* for deformed nuclei involving very few parameters. The most striking example of this is the prediction of a dominant $\beta \rightarrow \gamma$ branch which, although unrecognized up to now, has been shown in retrospect to arise naturally from the usual bandmixing formalism also; the origin of the dominance in the two approaches is, however, different, and it has been shown that the data for ^{168}Er support the existence of a direct $\Delta K = 2$ matrix element, as predicted by the IBA. Clearly this question deserves further study in other deformed nuclei. The two approaches, therefore, extractive and predictive, are complementary and the analytic techniques available in the geometrical framework can provide a powerful tool to study the source and magnitude of additional terms and perturbations that could be incorporated in the IBA treatment to perfect the description of a particular nucleus.

ACKNOWLEDGMENTS

Research has been performed under Contract DE-AC02-76CH00016 with the U.S. Department of Energy. We would like to express our appreciation to F. Iachello for numerous discussions and for his continued interest in this work. We are particularly grateful to L. L. Riedinger for his efforts in providing the derivations of the $\beta \rightarrow \gamma$ $B(E2)$ values incorporating three band mixing and for many enlightening and fruitful discussions concerning the band-mixing formalism. We would also like to thank O. Scholten for discussions and information concerning the two classes of terms giving rise to the $\beta \rightarrow \gamma$ matrix elements in the SU(3) limit of the IBA. Finally, we thank A. Bohr and B. R. Mottelson for the interest they have expressed in this work, for a useful exchange of ideas, and for suggestions concerning the aptness of the Mikhailov plot technique for comparing and contrasting the various theoretical approaches and the data.

[1]A. Arima and F. Iachello, Ann. Phys. (N.Y.) 99, 253 (1976); 111, 201 (1978); 123, 468 (1979); O. Scholten, F. Iachello, and A. Arima, *ibid.* 115, 325 (1978).

[2]R. F. Casten, in *Interacting Bose-Fermi Systems in Nuclei,* edited by F. Iachello, School Ettore Majorana, International Science Series (to be published).

[3]Aage Bohr and Ben R. Mottelson, *Nuclear Structure* (Benjamin, New York, 1975), Vol. 2.

[4]Aage Bohr and Ben R. Mottelson, Phys. Scr. 22, 468 (1980).

[5]R. F. Casten, D. D. Warner, M. L. Stelts, and W. F. Davidson, Phys. Rev. Lett. 45, 1077 (1980).

[6]R. F. Casten and J. A. Cizewski, Nucl. Phys. A309, 477 (1978).

[7]W. F. Davidson, D. D. Warner, R. F. Casten, K. Schreckenbach, H. G. Borner, J. Simic, M. Stojanovic, M. Bogdanovic, S. Koicki, W. Gelletly, G. B. Orr, and M. L. Stelts, J. Phys. G 7, 455 (1981); 7, 843 (1981).

[8]D. D. Warner, R. F. Casten, and W. F. Davidson, Phys. Rev. Lett. 45, 1761 (1980).

[9]O. Scholten (private communication).

[10]L. M. Greenwood, Nucl. Data Sheets 11, 385 (1974); J. M. Domingos, G. D. Symons, and A. C. Douglas, Nucl. Phys. A180, 600 (1972).

[11]M. A. Preston and R. K. Bhaduri, *Structure of the Nucleus* (Addison-Wesley, Reading, Massachusetts, 1975).

[12]Aage Bohr and Ben R. Mottelson (private communication).

[13]P. O. Tjøm and B. Elbek, Nucl. Phys. A107, 385 (1968).

[14]R. A. Harlan and R. K. Sheline, Phys. Rev. 160, 1005 (1967); D. G. Burke (private communication).

[15]K. Schreckenbach and W. Gelletly, Phys. Lett. 94B, 298 (1980).

[16]G. Alaga, K. Alder, A. Bohr, and B. R. Mottelson K. Dan Vidensk. Selsk. Mat.-Fys. Medd. 29, No. 9 (1955).

[17]W. Greiner, Nucl. Phys. 80, 417 (1966).

[18]L. L. Riedinger, N. R. Johnson, and J. H. Hamilton, Phys. Rev. 179, 1214 (1969).

[19]I. A. Fraser, J. S. Greenberg, S. H. Sie, R. G. Stokstad, G. A. Burginyon, and D. A. Bromley, Phys. Rev. Lett. 23, 1047 (1964).

[20]L. L. Riedinger, Ph. D. thesis, Vanderbilt University, 1969; and (private comunication).

[21]V. M. Mikhailov, Izv. Akad. Nauk Ser. Fiz. 30, 1334 (1966) [Bull. Acad. Sci. USSR Phys. Ser. 30, 1392 (1966)].

[22]R. C. Greenwood, C. W. Reich, H. A. Baader, H. R. Koch, D. Breitig, O. W. B. Schult, B. Fogelberg, A. Backlin, W. Mampe, T. von Egidy, and K. Schreckenbach, Nucl. Phys. A304, 327 (1978).

[23]W. Michaelis, H. Ottmar, and F. Weller, Nucl. Phys. A150, 161 (1970).

[24]H. R. Koch, Z. Phys. 192, 142 (1966).

[25]C. W. Reich, R. C. Greenwood, and R. A. Lokken, Nucl. Phys. A228, 365 (1974).